The Search for Gravitational Waves Via a Xylophone

M. Tinto
Communications Systems and Research Section

We discuss spacecraft Doppler tracking for detecting gravitational waves in which Doppler data recorded on the ground are linearly combined with Doppler measurements made on board a spacecraft. By using the four-link radio system first proposed by Vessot and Levine [1], we derive a new method for removing from the combined data the frequency fluctuations due to the Earth's troposphere, the Earth's ionosphere, and the mechanical vibrations of the antenna on the ground. This method also reduces the frequency fluctuations of the clock on board the spacecraft by several orders of magnitude at selected Fourier components.

The nonzero gravitational wave signal remaining at these frequencies makes this Doppler tracking technique the equivalent of a xylophone detector of gravitational radiation. Assuming calibration of the frequency fluctuations induced by the interplanetary plasma, a strain sensitivity equal to 4.7×10^{-18} at 10^{-3} Hz is estimated. Experiments of this kind could be performed (at minimal additional cost) with future interplanetary missions by adding instrumentation to the spacecraft payload and the ground station.

I. Introduction

The direct detection of gravitational waves is one of the most challenging experimental efforts in physics today. A successful observation of gravitational waves not only will represent a great triumph in experimental physics but will also provide a new observational tool for obtaining a better and deeper understanding about their sources as well as a unique test of the various proposed relativistic theories of gravity [2].

Since the first experiments by Joseph Weber [3] at the University of Maryland in the early sixties, designs for Earth-based as well as space-based detectors have been developed in the form of feasibility studies, prototypes, or fully operational instruments. Earth-based detectors, such as resonant bars and laser interferometers, are most sensitive to gravitational waves in the frequency band ranging from about 10 Hz to about 10 kHz, being limited below 10 Hz by seismic noise and above 10 kHz by instrumental noise [2]. Space-based detectors, such as the coherent microwave tracking of interplanetary spacecraft (S/C)[1] [4] and the proposed Michelson optical interferometers in planetary orbits [5,6], on the other hand, are most sensitive to a complementary band of frequencies, effectively in the range from about 10^{-5} Hz to about 1 Hz.

[1] F. B. Estabrook, *Proposal for Participation on Radio Science/Celestial Mechanics Team for an Investigation of Gravitational Radiation*, Galileo Project (unpublished internal document), Jet Propulsion Laboratory, Pasadena, California, 1976.

In present single-spacecraft Doppler tracking observations in particular, many of the noise sources can be either reduced or calibrated by implementing appropriate microwave frequency links and by using specialized electronics. The fundamental instrumental limitation is imposed by the frequency (time-keeping) fluctuations inherent to the reference clocks that control the microwave system [7]. Hydrogen maser clocks, currently used in Doppler tracking experiments, achieve their best performance at about a 1000-second integration time, with a fractional frequency stability of a few parts in 10^{-16}.[2] This is the reason why these interferometers in space are most sensitive to millihertz gravitational waves. This integration time is also comparable to the propagation time to spacecraft in the outer solar system. The frequency fluctuations induced by the intervening media have severely limited the sensitivities of these experiments. Among all the propagation noise sources, the troposphere is the largest and the hardest to calibrate to a reasonably low level. Its frequency fluctuations have been estimated to be as large as 10^{-13} at a 1000-second integration time [8].

It was shown by Armstrong that the effects of the troposphere could be reduced at selected Fourier frequencies by taking advantage of the sinusoidal behavior of its transfer function in the Doppler data [8]. In order to systematically remove the effect of the troposphere at any Fourier component, it was pointed out by Vessot and Levine [1] and Smarr et al. [9] that by adding to the spacecraft payload a highly stable frequency standard, a Doppler read-out system, and by utilizing a transponder at the ground antenna, one could make Doppler one-way (Earth–spacecraft and spacecraft–Earth) as well as two-way (spacecraft–Earth–spacecraft and Earth–spacecraft–Earth) measurements. This way of operation makes the Doppler link totally symmetric and allows, by properly combining the Doppler data recorded on the ground with the data measured on the spacecraft, the complete removal from the newly formed data of the frequency fluctuations due to the Earth's troposphere, the Earth's ionosphere, and the mechanical vibrations of the ground antenna. Their proposed scheme relied on the possibility of flying a hydrogen maser on a dedicated mission. Although current designs of hydrogen masers have demanding requirements in mass and power consumption, it seems very likely that by the beginning of the next century new space-qualified atomic clocks, with frequency stability of a few parts in 10^{-16} at a 1000-second integration time will be available. They would provide a sensitivity gain of almost a factor of one thousand with respect to the best-performance crystal-driven oscillators. Although this clearly would imply a great improvement in the technology of space-borne clocks, it would not allow us to reach a strain sensitivity better than a few parts in 10^{-16}. This sensitivity would be only a factor of five or ten better than the Doppler sensitivity expected to be achieved on the future Cassini project, a NASA mission to Saturn, which will take advantage of a high radio frequency link (32 GHz) in order to minimize the plasma noise and will use a water vapor radiometer purposely built for calibrating up to 95 percent of the frequency fluctuations due to the troposphere.[3]

In this article, we adopt the radio link configuration first envisioned by Vessot and Levine [1], but we combine the Doppler responses measured on board the spacecraft and on the ground in a different way, as will be shown in the following sections. In Section II, we derive the response functions of the one-way (Earth–spacecraft and spacecraft–Earth) as well as the two-way (Earth–spacecraft–Earth and spacecraft–Earth–spacecraft) Doppler tracking data measured on the ground and spacecraft. After describing the transfer functions of the noise sources affecting the sensitivities of these four data sets, we show that, in a properly chosen linear combination of the two one-way Doppler data, frequency fluctuations induced by the troposphere, ionosphere, and mechanical vibrations of the ground antenna can be removed at all times. We point out that our method is different from the one suggested by Vessot and Levine [1], Smarr et al. [9], and Piran et al. [10] in that it does utilize only one-way Doppler measurements (Earth–spacecraft and spacecraft–Earth). Furthermore, our technique allows us to reduce by several orders of magnitude, at selected Fourier components, the noise due to the clock on board the spacecraft. In Section III, we

[2] A. L. Riley, D. Antsos, J. W. Armstrong, P. Kinman, H. D. Wahlquist, B. Bertotti, G. Comoretto, B. Pernice, G. Carnicella, and R. Giordani, *Cassini Ka-Band Precision Doppler and Enhanced Telecommunications System Study* (internal document), Jet Propulsion Laboratory, Pasadena, California, January 22, 1990.

[3] Ibid.

estimate the strain sensitivity of this "xylophone" and find it to be equal to 4.7×10^{-18}, assuming the use of dual-frequency links for removing the frequency fluctuations induced by the interplanetary plasma and an observing time of 40 days. At this level of sensitivity, gravitational wave bursts, continuous signals of known frequency from selected sources, and a stochastic background of gravitational radiation should be detectable. Finally, in Section IV we present our comments and conclusions.

II. Doppler Tracking as a Xylophone Detector

In the Doppler tracking technique for searching for gravitational radiation, a distant interplanetary spacecraft is monitored from Earth through a radio link, and the Earth and the spacecraft act as free-falling test particles. A radio signal of nominal frequency ν_0 is transmitted to the spacecraft and coherently transponded back to Earth, where the received signal is compared to a signal referenced to a highly stable clock. Relative frequency changes $\Delta\nu/\nu_0$, as functions of time, are measured. When a gravitational wave crossing the solar system propagates through the radio link, it causes small perturbations in $\Delta\nu/\nu_0$, which are replicated three times in the Doppler data with maximum spacing given by the two-way light propagation time between the Earth and the spacecraft [7]. If we introduce a set of Cartesian orthogonal coordinates (X, Y, Z) in which the wave is propagating along the z-axis and (X, Y) are two orthogonal axes in the plane of the wave (see Fig. 1), then the Doppler response at time t can be written in the following form [7,8,11]:

$$\begin{aligned}\left(\frac{\Delta\nu(t)}{\nu_0}\right)_E \equiv E_2(t) = & -\frac{(1-\mu)}{2}h(t) - \mu\, h(t-(1+\mu)L) + \frac{(1+\mu)}{2}\, h(t-2L) \\ & + C_E(t-2L) - C_E(t) + 2B(t-L) + T(t-2L) + T(t) \\ & + A_E(t-2L) + A_{sc}(t-L) + TR_{sc}(t-L) + EL_{E_2}(t) + P_{E_2}(t) \qquad (1)\end{aligned}$$

where $h(t)$ is equal to

$$h(t) = h_+(t)\cos(2\phi) + h_\times(t)\sin(2\phi) \qquad (2)$$

Here, $h_+(t)$ and $h_\times(t)$ are the wave's two amplitudes with respect to the (X, Y) axis; (θ, ϕ) are the polar angles describing the location of the spacecraft with respect to the (X, Y, Z) coordinates; μ is equal to $\cos\theta$; and L is the distance to the spacecraft (units in which the speed of light $c = 1$).

We have denoted by $C_E(t)$ the random process associated with the frequency fluctuations of the clock on the Earth; $B(t)$ the joint effect of the noise from buffeting of the probe by nongravitational forces and from the antenna of the spacecraft; $T(t)$ the joint frequency fluctuations due to the troposphere, ionosphere, and ground antenna; $A_E(t)$ the noise of the radio transmitter on the ground; $A_{sc}(t)$ the noise of the radio transmitter on board; $TR_{sc}(t)$ the noise due to the spacecraft transponder; $EL_{E_2}(t)$ the noise from the electronics on the ground; and $P_{E_2}(t)$ the fluctuations due to the interplanetary plasma. Since the frequency fluctuations induced by the plasma are inversely proportional to the square of the radio frequency, by using high-frequency radio signals or by monitoring two different radio frequencies, which are transmitted to the spacecraft and coherently transmitted back to Earth, this noise source can be suppressed to very low levels or entirely removed from the data, respectively [12]. Searches for gravitational radiation with Doppler tracking utilizing only one radio frequency are usually performed around solar opposition in order to minimize the frequency fluctuations induced by the plasma [13]. The corresponding time scale during which data are recorded is about 40 days.

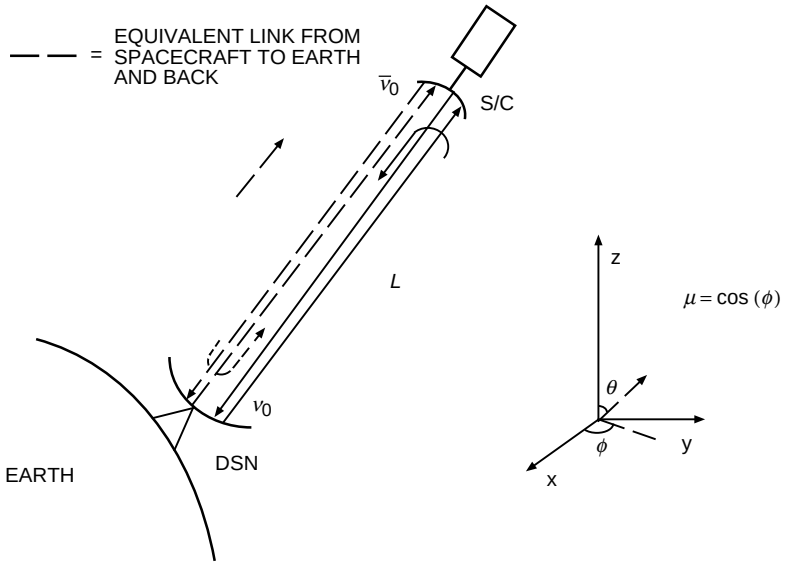

Fig. 1. A radio signal of nominal frequency ν_0 transmitted to a spacecraft and coherently transponded back to Earth. The gravitational wave train propagates along the z-direction, and the cosine of the angle between its direction of propagation and the radio beam is denoted μ. Together with two-way data, measurements of one-way Doppler can also be done by comparing the frequency of the received signal with the frequency generated by a local clock.

From Eq. (1), we deduce, to first order, that gravitational wave pulses of durations longer than the round-trip light time $2L$ give a Doppler response $E_2(t)$ that tends to zero. The tracking system essentially acts as a passband device, in which the low-frequency limit f_l is roughly equal to $(2L)^{-1}$ Hz, and the high-frequency limit f_H is set by the thermal noise in the receiver. Since the reference clock and some electronic components are most stable at integration times around 1000 seconds, Doppler tracking experiments are performed when the distance to the spacecraft is of the order of a few astronomical units (AU). This set the value of f_l for a typical experiment to about 10^{-4} Hz, while the thermal noise gives an f_H of about 3×10^{-2} Hz.

It is important to note the characteristic time signatures of the clock noise $C_E(t)$, of the probe antenna and buffeting noise $B(t)$, of the troposphere, ionosphere, and ground antenna noise $T(t)$, and of the transmitters $A_E(t)$ and $A_{sc}(t)$. The time signature of the clock noise can be understood by observing that the frequency of the signal received at time t contains clock fluctuations transmitted $2L$ seconds earlier. By subtracting from the received frequency the frequency of the radio signal transmitted at time t, we also subtract clock frequency fluctuations with the net result shown in Eq. (1) [8–10].

As far as the fluctuations due to the troposphere, ionosphere, and ground antenna are concerned, the frequency of the received signal is affected at the moment of reception as well as $2L$ seconds earlier. Since the frequency of the signal generated at time t does not yet contain any of these fluctuations, we conclude that $T(t)$ is positive-correlated at the round-trip light time $2L$ [8–10]. The time signature of the noises $B(t)$, $A_E(t)$, $A_{sc}(t)$, and $TR_{sc}(t)$ in Eq. (1) can be understood through similar considerations.

If a clock and Doppler readout system are added to the spacecraft radio instrumentation, and a transponder is installed at the ground station (Fig. 2), then one-way as well as two-way Doppler data can be recorded at the ground station and on board the spacecraft [1]. If we assume the Earth clock and the onboard clock to be synchronized and denote by $\overline{\nu}_0$ the frequency of the radio signal transmitted by the spacecraft, with $E_1(t)$ the one-way Doppler measured at time t at the station and with $S_1(t)$ and $S_2(t)$, respectively, the one-way and two-way Doppler measured on board the spacecraft at the

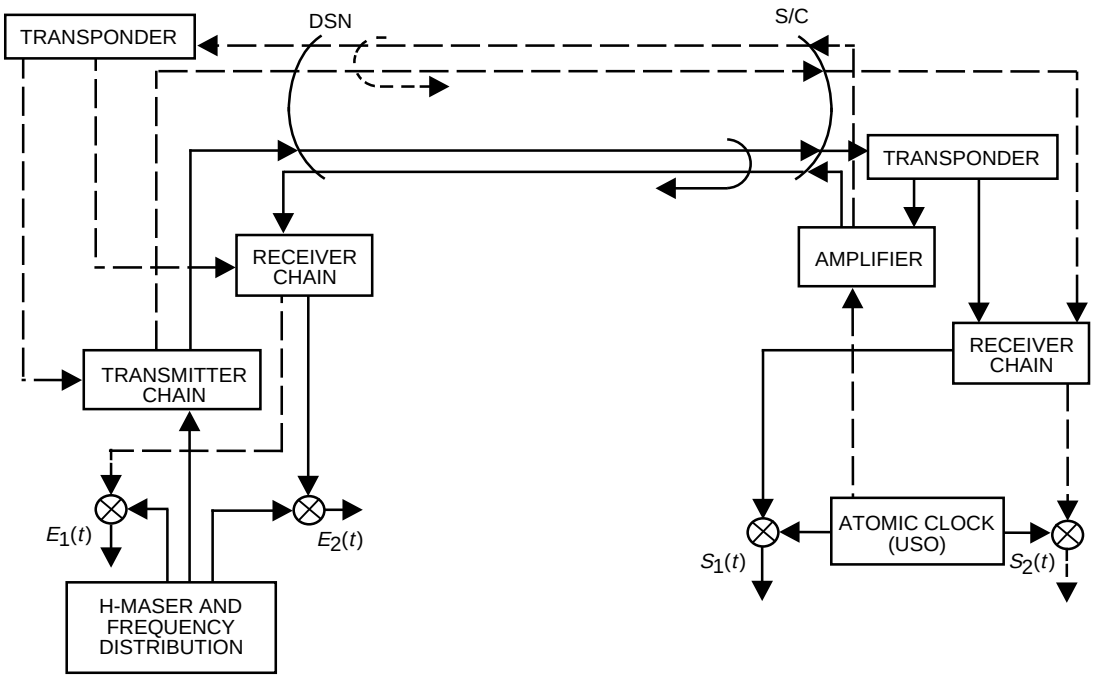

Fig. 2. The radio hardware at the ground antenna of the DSN and on board the spacecraft that allows the acquisition and recording of the four Doppler data, $E_1(t)$, $E_2(t)$, $S_1(t)$, and $S_2(t)$.

same time t, then a gravitational wave pulse appears in the Doppler data $E_1(t)$, $S_1(t)$, and $S_2(t)$ with the following signatures:

$$E_1(t) = \frac{(1-\mu)}{2}\left[h(t-(1+\mu)L) - h(t)\right] + C_{sc}(t-L) - C_E(t)$$
$$+ T(t) + B(t-L) + A_{sc}(t-L) + EL_{E_1}(t) + P_{E_1}(t) \tag{3}$$

$$S_1(t) = \frac{(1+\mu)}{2}\left[h(t-L) - h(t-\mu L)\right] + C_E(t-L) - C_{sc}(t)$$
$$+ T(t-L) + B(t) + A_E(t-L) + EL_{S_1}(t) + P_{S_1}(t) \tag{4}$$

$$S_2(t) = -\frac{(1+\mu)}{2}h(t-\mu L) + \mu h(t-L) + \frac{(1-\mu)}{2}h(t-2L-\mu L)$$
$$+ C_{sc}(t-2L) - C_{sc}(t) + B(t-2L) + B(t) + 2T(t-L)$$
$$+ A_{sc}(t-2L) + A_E(t-L) + TR_E(t-L) + EL_{S_2}(t) + P_{S_2}(t) \tag{5}$$

The gravitational wave signal in the Doppler responses can be derived using the method described in [7,14]. We have denoted by $C_{sc}(t)$ the random process associated with the frequency fluctuations of the onboard clock; $TR_E(t)$ the noise due to the transponder on the ground; $EL_{E_1}(t)$, $EL_{S_1}(t)$, and $EL_{S_2}(t)$ the noises from the electronics at the ground station and on the spacecraft in the one-way and two-way

data; and $P_{E_1}(t)$, $P_{S_1}(t)$, and $P_{S_2}(t)$ the fluctuations due to the interplanetary plasma. The frequency fluctuations due to the transmitters on the ground and on board have been denoted with the same random processes ($A_E(t)$ and $A_{sc}(t)$, respectively) we introduced in Eq. (1). This is correct as long as the two radio signals of frequencies ν_0 and $\overline{\nu}_0$ are amplified within the operational bandwidth (typically 40 to 50 MHz) of the same transmitters [15].[4,5] The Doppler data $S_1(t)$ and $S_2(t)$ are then time tagged and telemetered back to Earth in real time or at a later time during the mission.

It was first pointed out by Vessot and Levine [1] that by properly combining the four Doppler data it was possible to calibrate the frequency fluctuations of the troposphere, ionosphere, and ground antenna noise, $T(t)$. Their pioneering work, however, left open the question of whether there existed some other, perhaps more complicated, linear combinations of the Doppler data that would further improve the sensitivity of Doppler tracking. In what follows, we answer this question and derive a method that allows us to uniquely identify such a combination of the data.

Let $\widetilde{E_1}(f)$ be the Fourier transform of the time series $E_1(t)$:

$$\widetilde{E_1}(f) \equiv \int_{-\infty}^{+\infty} E_1(t) e^{2\pi i f t} dt \tag{6}$$

and similarly let us denote by $\widetilde{E_2}(f)$, $\widetilde{S_1}(f)$, and $\widetilde{S_2}(f)$ the Fourier transforms of $E_2(t)$, $S_1(t)$, and $S_2(t)$, respectively. The most general linear combination of the four Doppler data given in Eqs. (1), (3), (4), and (5) can be written in the Fourier domain as follows:

$$\widetilde{y}(f) \equiv a(f,L)\widetilde{E_1}(f) + b(f,L)\widetilde{E_2}(f) + c(f,L)\widetilde{S_1}(f) + d(f,L)\widetilde{S_2}(f) \tag{7}$$

where $a(f,L)$, $b(f,L)$, $c(f,L)$, and $d(f,L)$ are, for the moment, arbitrary functions of the Fourier frequency, f, and the distance to the spacecraft, L.

If we substitute the Fourier transforms of Eqs. (1), (3), (4), and (5) into Eq. (7), we get the following expression for $\widetilde{y}(f)$:

$$\begin{aligned}
\widetilde{y}(f) = {} & \widetilde{H}(f) + \widetilde{\overline{C_E}}(f) + \widetilde{\overline{C_{sc}}}(f) + \widetilde{\overline{T}}(f) + \widetilde{\overline{B}}(f) + \widetilde{\overline{A_E}}(f) + \widetilde{\overline{A_{sc}}}(f) \\
& + a\left[\widetilde{EL_{E_1}}(f) + \widetilde{P_{E_1}}(f)\right] + b\left[\widetilde{TR_{sc}}(f)e^{2\pi i f L} + \widetilde{EL_{E_2}}(f) + \widetilde{P_{E_2}}(f)\right] \\
& + c\left[\widetilde{EL_{S_1}}(f) + \widetilde{P_{S_1}}(f)\right] + d\left[\widetilde{TR_E}(f)e^{2\pi i f L} + \widetilde{EL_{S_2}}(f) + \widetilde{P_{S_2}}(f)\right]
\end{aligned} \tag{8}$$

where we have denoted by $\widetilde{H}(f)$, $\widetilde{\overline{C_E}}(f)$, $\widetilde{\overline{C_{sc}}}(f)$, $\widetilde{\overline{T}}(f)$, $\widetilde{\overline{B}}(f)$, $\widetilde{\overline{A_E}}(f)$, and $\widetilde{\overline{A_{sc}}}(f)$ the following expressions:

---

[4] J. W. Armstrong, personal communication, Jet Propulsion Laboratory, Pasadena, California, 1995.

[5] R. Perez, "DSS 15 20 kW X-Band Transmitter Test Results Regarding Stability Requirements," JPL Interoffice Memorandum 3337-89-098, Jet Propulsion Laboratory, Pasadena, California, October 3, 1989.

$$\widetilde{H}(f) = \Big\{ a\,\frac{(1-\mu)}{2}\left[e^{2\pi i f(1+\mu)L} - 1\right] + b\left[\frac{(\mu-1)}{2} - \mu e^{2\pi i f(1+\mu)L} + \frac{(1+\mu)}{2}e^{4\pi i f L}\right]$$

$$+\; c\,\frac{(1+\mu)}{2}\left[e^{2\pi i f L} - e^{2\pi i f \mu L}\right] + d\left[-\frac{(\mu+1)}{2}e^{2\pi i f \mu L} + \mu e^{2\pi i f L}\right.$$

$$\left. +\; \frac{(1-\mu)}{2}e^{2\pi i f(2+\mu)L}\right]\Big\}\,\widetilde{h}(f) \tag{9}$$

$$\widetilde{\overline{C_E}}(f) = \widetilde{C_E}(f)\left[-a + b\left(e^{4\pi i f L} - 1\right) + c e^{2\pi i f L}\right] \tag{10}$$

$$\widetilde{\overline{C_{sc}}}(f) = \widetilde{C_{sc}}(f)\left[a e^{2\pi i f L} - c + d\left(e^{4\pi i f L} - 1\right)\right] \tag{11}$$

$$\widetilde{\overline{T}}(f) = \widetilde{T}(f)\left[a + b\left(e^{4\pi i f L} + 1\right) + c e^{2\pi i f L} + 2d e^{2\pi i f L}\right] \tag{12}$$

$$\widetilde{\overline{B}}(f) = \widetilde{B}(f)\left[a e^{2\pi i f L} + 2b e^{2\pi i f L} + c + d\left(e^{4\pi i f L} + 1\right)\right] \tag{13}$$

$$\widetilde{\overline{A_E}}(f) = \widetilde{A_E}(f)\left[b e^{4\pi i f L} + c e^{2\pi i f L} + d e^{2\pi i f L}\right] \tag{14}$$

$$\widetilde{\overline{A_{sc}}}(f) = \widetilde{A_{sc}}(f)\left[a e^{2\pi i f L} + b e^{2\pi i f L} + d e^{4\pi i f L}\right] \tag{15}$$

The four functions a, b, c, and d can be determined by requiring that the transfer functions entering into the random processes given in Eqs. (10) through (15) are simultaneously equal to zero, and by further checking that each solution provides a nonzero gravitational wave signal in the corresponding combined data. This condition implies that a, b, c, and d must satisfy a homogeneous linear system of six equations in four unknowns. We calculated the rank of the (6×4) matrix associated with this linear system by using the algebraic computer language *Mathematica*, and we found it to be equal to two. The corresponding solution can be written in the following form:

$$a(f,L) = c(f,L)e^{-2\pi i f L} - d(f,L)\left[e^{2\pi i f L} - e^{-2\pi i f L}\right] \tag{16}$$

$$b(f,L) = -c(f,L)e^{-2\pi i f L} - d(f,L)e^{-2\pi i f L} \tag{17}$$

where c and d can be any arbitrary complex functions of f and L not simultaneously equal to zero. If we substitute Eq. (17) into Eq. (9), however, we also find that the gravitational wave signal $\widetilde{H}(f)$ vanishes. In other words, any linear combination of the four Doppler data that does not contain any clocks, troposphere, ionosphere, mechanical vibrations of the ground antenna, buffeting of the spacecraft, and transmitter noise also has a null response to a gravitational wave pulse. These results imply that, at any Fourier frequency f, we can remove only one of the considered noise sources. Among all the noise sources affecting spacecraft Doppler tracking, the frequency fluctuations due to the troposphere, ionosphere, and mechanical vibrations of the ground antenna, $\widetilde{T}(f)$, are the largest. If we choose a, b,

c, and d in such a way that the transfer function of $\widetilde{T}(f)$ in the combined data is equal to zero, from Eq. (12) we find that a, b, c, and d must satisfy the following condition:

$$a(f,L) = -b(f,L)\left[e^{4\pi i f L}+1\right] - c(f,L)e^{2\pi i f L} - 2d(f,L)e^{2\pi i f L} \tag{18}$$

Since b, c, and d cannot be equal to zero simultaneously, we will choose c to be equal to $1/2$ and b and d to be equal to zero. In other words, we will consider only linear combinations of one-way Doppler data. Note that with this choice we eliminate from the combined data $y(t)$ the frequency fluctuations due to the transponders and the interplanetary plasma that affect the two-way Doppler data. These considerations imply the following expression for $\widetilde{y}(f)$:

$$\widetilde{y}(f) = \frac{1}{2}\left[\widetilde{S_1}(f) - \widetilde{E_1}(f)e^{2\pi i f L}\right] \tag{19}$$

If we substitute the Fourier transforms of Eqs. (3) and (4) into Eq. (19), we get

$$\begin{aligned}
\widetilde{y}(f) = {} & \frac{e^{2\pi i f L}}{2}\left[1 - \frac{(1+\mu)}{2}e^{2\pi i f(\mu-1)L} - \frac{(1-\mu)}{2}e^{2\pi i f(\mu+1)L}\right]\widetilde{h}(f) \\
& + \widetilde{C_E}(f)\; e^{2\pi i f L} - \frac{1}{2}\widetilde{C_{sc}}(f)\left[e^{4\pi i f L}+1\right] + \frac{1}{2}\widetilde{B}(f)\left[1 - e^{4\pi i f L}\right] \\
& + \frac{e^{2\pi i f L}}{2}\left[\widetilde{A_E}(f) - \widetilde{A_{sc}}(f)e^{2\pi i f L}\right] + \frac{1}{2}\;\left[\widetilde{P_{S_1}}(f) \;-\; \widetilde{P_{E_1}}(f)e^{2\pi i f L}\right] \\
& + \frac{1}{2}\left[\widetilde{EL_{S_1}}(f) - \widetilde{EL_{E_1}}(f)e^{2\pi i f L}\right]
\end{aligned} \tag{20}$$

Among all the remaining noise sources included in Eq. (20), the frequency fluctuations due to the clock on board the spacecraft are expected to be the largest. The frequency stability of a crystal-driven oscillator, like the one built for the Cassini mission, for instance, has been measured to be equal to 9.5×10^{-14} at a 1000-second integration time, making this clock the most stable space-qualified reference frequency ever built; it is called an ultra stable oscillator (USO). Advances in the field of space-based metrology suggest that by the beginning of the next century space-qualified atomic clocks with sensitivities comparable to ground-based clocks will be available [16].

For the moment, we will not make any assumptions on the frequency stability of the clock on board and will return to this point later. We will focus instead on the structure of the noise sources shown in Eq. (20). We note that the transfer function of the onboard clock noise is equal to zero at frequencies that are multiple odd integers of the inverse of twice the round-trip light time. If we denote by δ the time interval over which the Doppler data are recorded (typically 40 days), the frequency resolution Δf of the data will be equal to $1/\delta$. This implies that the frequency fluctuations of the clock on board can be minimized at the following frequencies:

$$f_k = \frac{(2k-1)}{4L} \pm \frac{\Delta f}{2}, \qquad k = 1, 2, 3, \cdots \tag{21}$$

At these frequencies, and to first order in $\Delta f\; L$, the Doppler response $\widetilde{y}(f_k)$ is equal to

$$\widetilde{y}(f_k) \approx \frac{i}{2}(-1)^k \left[-1 + i\mu e^{(\pi/2)i\mu(2k-1)}(-1)^k\right] \widetilde{h}(f) + i(-1)^{k+1}\widetilde{C_E}(f_k) \pm (\pi i \Delta f L)\widetilde{C_{sc}}(f_k)$$

$$+ \widetilde{B}(f_k) + \frac{1}{2}\left[\widetilde{EL_{S_1}}(f_k) - i\widetilde{EL_{E_1}}(f_k)(-1)^{k+1}\right] + \frac{1}{2}\left[\widetilde{P_{S_1}}(f_k) - i\widetilde{P_{E_1}}(f_k)(-1)^{k+1}\right]$$

$$+ \frac{1}{2}(-1)^{k+1}\left[i\widetilde{A_E}(f_k) + \widetilde{A_{sc}}(f_k)(-1)^{k+1}\right] \tag{22}$$

If we assume a spacecraft distance L equal to 10 AU and a tracking time δ of 40 days, we find that

$$\frac{\pi \Delta f L}{c} = 4.7 \times 10^{-3} \tag{23}$$

In other words, at frequencies that are multiple odd integers of the inverse of twice the round-trip light time to a spacecraft out to 10 AU, the noise of the onboard clock is reduced by about three orders of magnitude. This Doppler tracking technique can be regarded as a xylophone detector of gravitational waves, having around fifty "resonant" frequencies in the frequency band of a typical Doppler experiment. We should point out, however, that these resonant frequencies in general will not be constant, since the distance to the spacecraft will change over a time interval of 40 days. As an example, however, let us assume again $L = 10$ AU, $\delta = 40$ days, and $f = 5 \times 10^{-5}$ Hz. The variation in spacecraft distance corresponding to a frequency change equal to the resolution bin width (3×10^{-7} Hz) is equal to 9.0×10^6 km. Trajectory configurations fulfilling a requirement compatible to the one just derived have been observed during past spacecraft missions[6] and, therefore, we do not expect this to be a limiting factor. The xylophone technique, namely the idea of looking at selected Fourier components where the transfer functions of some Doppler noise sources are null, has already been implemented successfully by Armstrong [8] in regular spacecraft Doppler searches for gravitational waves. In that case, however, he could reduce by several orders of magnitude at selected Fourier frequencies only the fluctuations due to the troposphere, ionosphere, and ground antenna, $T(t)$.

In Eq. (22) we also provide the antenna pattern of the remaining gravitational wave signal in the combined data. This is equal to zero when $\mu = \pm 1$ and has a maximum value of $1/2$ at $\mu = 0$. For sources randomly distributed over the sky, as in the case of a stochastic background of gravitational waves, we can assume the angles (θ, ϕ) to be random variables uniformly distributed over the sphere and over the interval $[0, 2\pi]$, respectively. The average over (θ, ϕ) of the antenna pattern given in Eq. (22) is equal to zero, while its variance, which we will denote with $\sigma_h^2(k)$, is equal to the following monotonically increasing function of the integer k:

$$\sigma_h^2(k) = \frac{1}{3} - \frac{2}{\pi^2(2k-1)^2}, \qquad k = 1, 2, 3, \cdots \tag{24}$$

Before concluding this section, we note that, together with the Doppler data $y(t)$, we can also use as veto any combined data determined by the functions $a(f, L)$, $b(f, L)$, $c(f, L)$, and $d(f, L)$ satisfying Eqs. (16) and (17). These data have the important property of having zero response to a gravitational wave. By comparing the output of the two data sets at each xylophone frequency, we will be able to discriminate real gravitational wave signals against random-noise fluctuations. We will quantitatively analyze in a forthcoming article the improvement in likelihood of detection provided by the use of veto data in xylophone searches for gravitational wave pulses.

[6] J. W. Armstrong, op cit.

III. Expected Sensitivities

From Eq. (22), we can estimate the expected root-mean-squared (rms) noise level $\sigma(f_k)$ of the frequency fluctuations in the bins of width Δf, around the frequencies $f_k (k = 1, 2, 3, \cdots)$. This is given by the following expression:

$$\sigma(f_k) = [S_y(f_k)\Delta f]^{1/2}\,, \qquad k = 1, 2, 3, \cdots \tag{25}$$

where $S_y(f_k)$ is the one-sided power spectral density of the noise sources in the Doppler response $y(t)$ at the frequency f_k. In what follows, we will assume that the random processes representing these noises are uncorrelated with each other and their one-sided power spectral densities are as given in Table 1. The Allan deviation at a given integration time τ is a statistical parameter for describing frequency stability. It represents the rms expectation value of the random process associated with the fractional frequency changes, between time-contiguous frequency measurements, each made over time intervals of duration τ. In this table, we have assumed a frequency stability of 1.0×10^{-16} at a 1000-second integration time for the clock at the ground station. Although this is a factor of four better than what has been measured so far,[7] it seems very likely that by the beginning of the next century such sensitivity will be achievable. As far as the other sensitivity figures provided in Table 1 are concerned, they are as given by Riley et al.[8] This document is a summary of a detailed study, performed jointly by scientists and engineers of NASA's Jet Propulsion Laboratory and the Italian Space Agency (ASI) Alenia Spazio, for assessing the magnitude and spectral characteristics of the noise sources that will determine the Doppler sensitivity of the future gravitational wave experiment on the Cassini mission. Also included in Table 1 is the spectral density of the noise of a crystal-driven USO. A description of the radio hardware used for implementing a xylophone detector, schematically represented in Fig. 2, is given in the Appendix.

Table 1. The noise sources entering into the combined Doppler response *y(t)*.

Error source	Allan deviation at 1000 s	Fractional frequency one-sided power spectral density
One-way plasma (Ka-band)	4.9×10^{-16}	$2.7 \times 10^{-30} f^{-2/3}$
H-maser	1.0×10^{-16}	$6.2 \times \left(10^{-28} f + 10^{-33} f^{-1} + 10^{-30}\right)$
Frequency distribution	1.0×10^{-17}	$1.3 \times 10^{-26} f^2$
Receiver chain	3.1×10^{-17}	$1.3 \times 10^{-25} f^2$
Transmitter chain	3.4×10^{-16}	2.3×10^{-28}
Thermal noise	3.8×10^{-17}	$1.9 \times 10^{-25} f^2$
Spacecraft antenna and buffeting	5.8×10^{-17}	$5.0 \times 10^{-42} f^{-3} + 10^{-31} + 5.0 \times 10^{-30}$
Spacecraft amplifier	5.0×10^{-17}	$4.0 \times 10^{-27} f$
USO	9.5×10^{-14}	$6.5 \times 10^{-27} f^{-1}$

If dual radio frequencies in the uplink and downlink are used, then the frequency fluctuations due to the interplanetary plasma can be entirely removed [12]. We will refer to this configuration as Mode I. If instead only one frequency is adopted, which we will assume to be Ka-band (32 GHz), we will refer to this configuration as Mode II. It is planned that Ka-band will be used on most of the forthcoming NASA missions and will be implemented on the ground antennas of the Deep Space Network (DSN) by the year 1999 for the Cassini mission.

[7] A. L. Riley et al., op cit.

[8] A. L. Riley et al., op. cit.

In Fig. 3, we plot the rms $\sigma(f_k)$ of the noise as a function of the frequencies $f_k (k = 1, 2, 3, \cdots)$, assuming that an interplanetary spacecraft is out to a distance $L = 1.0$ AU. For this configuration, the fundamental frequency of the xylophone [Eq. (21)] is equal to 5×10^{-4} Hz. The Mode I configuration is represented by two curves, depending on whether an atomic clock (circles) or a USO (squares) is operated on board the spacecraft. Sensitivity curves for the Mode II configuration are also provided, again with an atomic clock on board (up triangles) or a USO (down triangles). The best sensitivity is achieved in the Mode I configuration, regardless of whether an atomic clock or a USO is operated on board the spacecraft (circles and squares are superimposed). This is because the noise of the clock on board is reduced in amplitude by a factor $\pi \Delta f L/c = 4.8 \times 10^{-4}$ at the xylophone frequencies. At the Fourier frequency $f = 1.5 \times 10^{-3}$ Hz, the corresponding rms noise level is equal to 4.7×10^{-18}, and it increases to a value of 5.7×10^{-18} at $f = 10^{-2}$ Hz. As far as the Mode II configuration is concerned, the rms noise level is equal to 7.9×10^{-18} at $f = 1.5 \times 10^{-3}$ Hz, while it decreases to 6.3×10^{-18} at $f = 10^{-2}$ Hz. This is due to the fact that the one-sided power spectral density of the fractional frequency fluctuations due to the interplanetary plasma decays as $f^{-2/3}$.

In Fig. 4, we analyze the configuration with a spacecraft out to a distance $L = 5$ AU and a corresponding fundamental frequency of the xylophone equal to $f = 10^{-4}$ Hz. At this frequency, with the plasma noise totally calibrated and by operating an atomic clock on the spacecraft, we find a sensitivity equal to 6.4×10^{-18}. At $f = 10^{-3}$ Hz, the sensitivity is again equal to 4.7×10^{-18}, and it slightly increases at $f = 10^{-2}$ Hz. The sensitivity figures with plasma calibrations with a USO on board (squares) are significantly larger than those corresponding to the configuration with an atomic clock (circles). As the distance to the spacecraft increases, the noise of the onboard clock increases proportionally at the xylophone frequencies. Consequently, the noise of the USO begins to dominate over the noise of the atomic clock at those frequencies. The minimum of the curve is equal to 5.1×10^{-18} at $f = 4.0 \times 10^{-3}$ Hz, while at $f = 10^{-4}$ Hz and $f = 10^{-2}$ Hz, the sensitivities are equal to 1.2×10^{-17} and 5.6×10^{-18}, respectively. In the Mode II configuration, the two sensitivity curves (up triangles and down triangles) are almost identical, with an optimal sensitivity at $f = 1.0 \times 10^{-2}$ Hz equal to 6.3×10^{-18}.

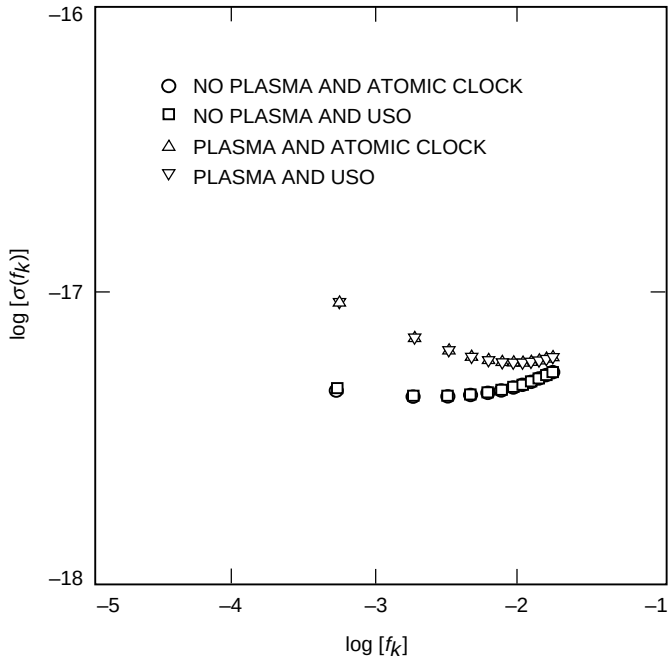

Fig. 3. The rms noise level as a function of the frequencies f_k (k = 1,2,3,···), estimated for a spacecraft that is out to a distance L = 1.0 AU.

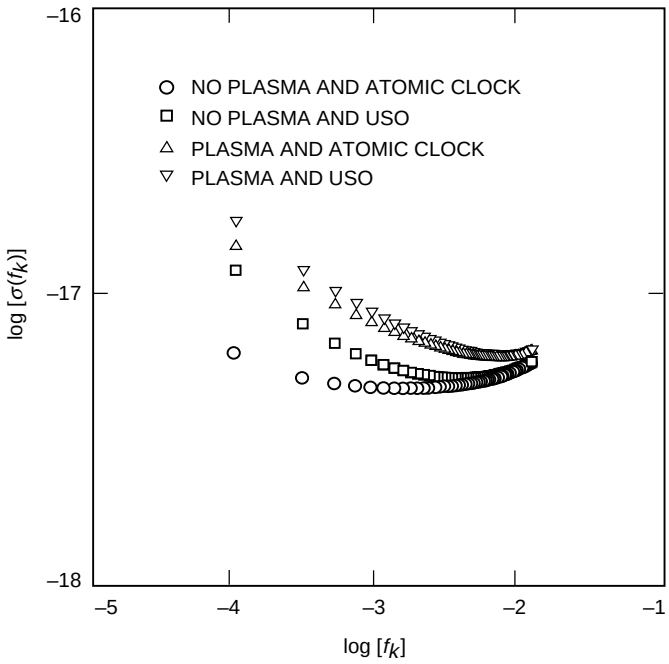

Fig. 4. The rms noise level as a function of the frequencies f_k (k = 1,2,3,···), estimated for a spacecraft that is out to a distance L = 5 AU.

Finally, in Fig. 5 we analyze the configuration of a spacecraft out to $L = 10$ AU, with a corresponding lowest xylophone frequency equal to 5×10^{-5} Hz. In this case, an atomic reference frequency on board gives a significantly better sensitivity than the one achievable with a USO in the low-frequency region of the accessible bandwidth. We estimate a strain sensitivity of 8.3×10^{-18} at $f = 5 \times 10^{-5}$ Hz. As we move to the high-frequency region, the sensitivity gets to its minimum of 4.7×10^{-18} at 1.6×10^{-3} Hz (circles). Note that in the low-frequency region the sensitivities of the configuration with plasma calibration and USO on board are worse than those in which the plasma is not calibrated and an atomic frequency reference is used on the spacecraft. This is because the one-sided power spectral density of the fractional frequency fluctuations of the USO decreases as f^{-1}, while that of the plasma goes as $f^{-2/3}$.

We note, as a summary to the results presented above, that the sensitivity value of 4.7×10^{-18} at $f = 10^{-3}$ Hz is determined essentially by the noise due to the transmitter chain (see Table 1). The one-sided power spectral density of the relative frequency fluctuations due to the transmitter chain is independent of the Fourier frequency and at $f = 10^{-3}$ Hz is about two orders of magnitude larger than the one-sided power spectral densities of the remaining noise sources given in Table 1. Research and development are in progress at the Jet Propulsion Laboratory in order to further reduce this noise source to smaller values [15].[9]

As a consequence of the intrinsic narrowband nature of the xylophone detector, the most likely sources of gravitational waves it will be able to detect will be broadband bursts and a stochastic background of gravitational radiation. A complete and accurate review of these sources, and estimates of the corresponding event rates of interest in the frequency band of the xylophone, are given in [2]. Here we will briefly summarize some of the anticipated sources of gravitational waves and compare the amplitude of the waves they are expected to radiate to the estimated rms noise levels derived in the previous section. A complete analysis of how further to improve the sensitivity by optimally filtering the data when searching for these signals will be the subject of a forthcoming article.

[9] R. Perez, op cit.

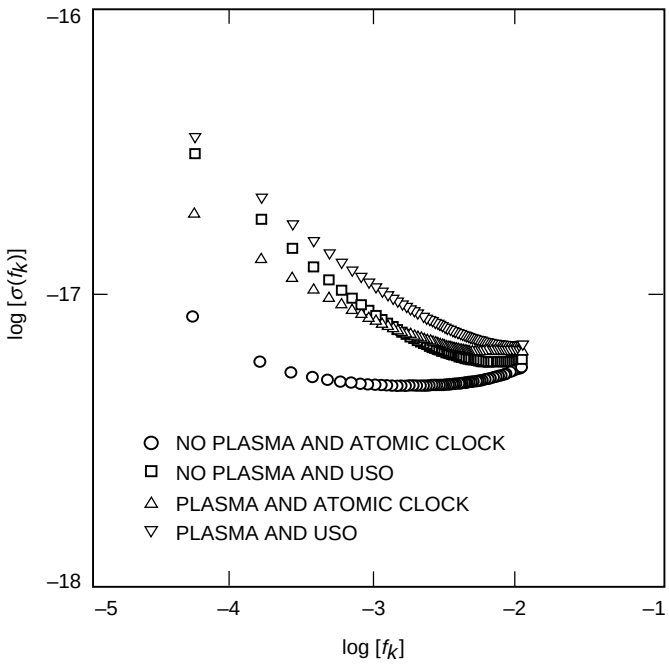

Fig. 5. The rms noise level as a function of the frequencies f_k (k = 1,2,3,···), estimated for a spacecraft that is out to a distance L = 10 AU.

A collapse of a star cluster to form a super massive black hole would radiate at 10^{-3} Hz and out to 0.5 Gpc a signal of characteristic wave amplitude equal to 2.0×10^{-17}, assuming that the energy emitted in the form of gravitational radiation is 10^{-4} times the rest mass of the system. Such a signal would be about 2.1 times the rms noise level we expect to achieve with the xylophone at the same frequency if we assume the direction of propagation of the wave to be orthogonal to the radio link. More optimistic assumptions on the efficiency of the energy radiated [2], in which this could be as much as 10^{-2} times the rest mass of the system, would imply a signal-to-noise ratio of 21 at $f = 10^{-3}$ Hz, again at the maximum antenna pattern. Out to 0.5 Gpc, it is conceivable that the event rate could be sufficiently high for a successful observation during the 40 days of tracking, although to our knowledge there are no published estimates on this issue.

The fall of small black holes into super massive black holes, like what might happen at the end of the merger of two galaxies hosting at their centers a black hole, would give origin to a potentially detectable gravitational radiation. In the scenario in which the larger hole has a mass of 10^7 solar masses and the mass of the other hole is 10^4 solar masses, at 10^{-3} Hz and out to the Virgo cluster of galaxies, the burst emitted during the merger would be observable by the xylophone with a signal-to-noise ratio of about 2. The Virgo cluster, with its 1000 galaxies, could provide a high event rate of such signals, taking into account the indirect evidence of the existence of a super massive black hole at the center of the galaxy M87 [2].

When searching for a stochastic background of gravitational radiation, a xylophone sensitivity equal to 4.7×10^{-18} at 10^{-3} Hz implies an energy density per unit logarithmic frequency and per unit critical energy density Ω [2] equal to 1.0×10^{-4}, after taking into account the effect of the rms antenna pattern $\sigma_h(k = 1)$ given in Eq. (24). If, however, we consider a sensitivity of 8.3×10^{-18} achievable at $f = 5 \times 10^{-5}$ with a spacecraft out to $L = 10$ AU and tracked with dual frequency for calibrating the frequency fluctuations due to the interplanetary plasma (Fig. 5), we find an Ω equal to 7.9×10^{-7}. Since several astrophysical sources of a gravitational wave background, like first-order cosmological phase transitions

or cosmic strings, are expected to give an Ω of about 10^{-6}, we conclude that the xylophone should be able to validate or disprove in a unique way the existence of such sources of background radiation.

The six known white-dwarf binary systems in our galaxy are expected to emit an almost monochromatic radiation of an amplitude smaller than the best rms noise level the xylophone can achieve [2]. However, performing a fine-tuned search for the continuous radiation from such systems during spacecraft cruise, when the inverse of twice the round-trip light time (or its harmonics) coincides with the estimated wave's frequency, would allow an important test of the predictions of general relativity and establish a significant benchmark sensitivity level for future planned space-based interferometers [5,6].

Besides known galactic binary systems, we could make an all-sky search at the xylophone frequencies for sinusoidal gravitational waves from binary systems containing black holes. A binary system in the Virgo cluster, with two black holes of masses equal to 10^4 solar masses, would radiate a continuous signal of a characteristic amplitude equal to 2.0×10^{-16} at 10^{-3} Hz. This signal would generate a maximum response of the xylophone at this frequency equal to 21.3 times the estimated rms noise level.

IV. Conclusions

We have discussed a method for significantly increasing the sensitivity of Doppler tracking experiments aimed at the detection of gravitational waves. The main result of our analysis, deduced in Eq. (22), shows that by flying a frequency reference and by adding a Doppler extractor on board the spacecraft and a transponder at the DSN antenna, we can achieve at selected Fourier components a strain sensitivity of 4.7×10^{-18}. This sensitivity figure is obtained by completely removing the frequency fluctuations due to the interplanetary plasma, at a Fourier frequency equal to 10^{-3} Hz. Our method relies on a properly chosen linear combination of the one-way Doppler data recorded on board with those measured on the ground. It allows us to remove entirely the frequency fluctuations due to the troposphere, ionosphere, and antenna mechanical vibrations, and for a spacecraft that is tracked for 40 days out to 1 AU, it reduces by almost four orders of magnitude the noise due to the onboard clock.

The experimental technique presented in this article can be extended to a configuration with two spacecraft tracking each other through a microwave or a laser link. Future space-based laser interferometric detectors of gravitational waves [5,6], for instance, could implement this technique as a backup option if failure of some of their components made normal interferometric operation impossible.

As a final note, a method similar to the one presented can be used in all the classic tests of the relativistic theory of gravity in which one-way and two-way spacecraft Doppler measurements are used as primary data sets. We will analyze the implications of the sensitivity improvements that this technique will provide for direct measurements of quantities such as the gravitational red shift, the second-order relativistic Doppler effect predicted by the theory of special relativity, searches for possible anisotropy in the velocity of light, measurements of the parameterized post-Newtonian parameters, and measurements of the deflection and time delay of radio signals by the sun. This research is in progress and will be the subject of a forthcoming article.

Acknowledgments

It is a pleasure to thank John D. Anderson, John W. Armstrong, Sami W. Asmar, Frank B. Estabrook, and Luciano Iess for several useful discussions and their encouragement during this work.

References

[1] R. F. C. Vessot and M. W. Levine, "A Test of the Equivalence Principle Using a Space-Borne Clock," *Gen. Relativ. Gravit.*, vol. 10, no. 3, pp. 181–204, 1979.

[2] K. S. Thorne, "Gravitational Radiation," *Three Hundred Years of Gravitation*, edited by S. W. Hawking and W. Israel, Cambridge, United Kingdom: Cambridge University Press, 1987.

[3] J. Weber, "Detection and Generation of Gravitational Waves," *Phys. Rev.*, vol. 117, no. 1, pp. 306–313, 1960.

[4] F. B. Estabrook, R. W. Hellings, H. D. Wahlquist, J. D. Anderson, and R. S. Wolff, "Spacecraft Doppler Tracking and Gravitational Radiation," *Sources of Gravitational Radiation*, edited by L. Smarr, Cambridge, United Kingdom: Cambridge University Press, 1979.

[5] Max-Planck-Institute für Quantenoptic, *LISA: (Laser Interferometer Space Antenna) Proposal for a Laser-Interferometric Gravitational Wave Detector in Space*, vol. MPQ 177, Garching bei München, Germany, 1993.

[6] J. E. Faller, P. L. Bender, J. L. Hall, D. Hils, R. T. Stebbins, and M. A. Vincent, "An Antenna for Laser Gravitational Wave Observations in Space," *Adv. Space Res.*, vol. 9, no. 9, pp. 107–111, 1989.

[7] F. B. Estabrook and H. D. Wahlquist, "Response of Doppler Spacecraft Tracking to Gravitational Radiation," *Gen. Relativ. Gravit.*, vol. 6, no. 5, pp. 439–447, 1975.

[8] J. W. Armstrong, "Spacecraft Gravitational Wave Experiments," *Gravitational Wave Data Analysis*, edited by B. F. Schutz, Dordrecht, Netherlands: Kluwer, p. 153, 1989.

[9] L. L. Smarr, R. F. C. Vessot, C. A. Lundquist, R. Decher, and T. Piran, "Gravitational Waves and Red Shifts: A Space Experiment for Testing Relativistic Gravity Using Multiple Time-Correlated Radio Signals," *Gen. Relativ. Gravit.* vol. 15, no. 2, pp. 129–163, 1983.

[10] T. Piran, E. Reiter, W. G. Unruh, and R. F. C. Vessot, "Filtering of Spacecraft Doppler Tracking Data and Detection of Gravitational Radiation," *Phys. Rev. D*, vol. 34, no. 4, pp. 984–990, 1986.

[11] M. Tinto and J. W. Armstrong, "Coincidence Probabilities for Spacecraft Gravitational Wave Experiments: Massive Coalescing Binaries," *The Astrophysical Journal*, vol. 372, no. 5, pp. 545–553, 1991.

[12] B. Bertotti, G. Comoretto, and L. Iess, "Doppler Tracking of Spacecraft With Multifrequency Links," *Astron. Astrophys.*, vol. 269, no. 7, pp. 608–616, 1993.

[13] J. W. Armstrong, R. Woo, and F. B. Estabrook, "Interplanetary Phase Scintillation and the Search for Very Low Frequency Gravitational Radiation," *The Astrophysical Journal*, vol. 230, no. 6, pp. 570–574, 1979.

[14] M. Tinto and F. B. Estabrook, "Parallel Beam Interferometric Detectors of Gravitational Waves," *Phys. Rev. D*, vol. 52, no. 4, pp. 1749–1754, 1995.

[15] B. L. Conroy and D. Lee, "Measurements of Allan Variance and Phase Noise at Fractions of a Millihertz," *Rev. Sci. Instrum.*, vol. 61, no. 6, pp. 1720–1723, 1990.

[16] R. F. C. Vessot, "Experimental Techniques With Highly Stable Clocks," *Proceedings of the XIVth Moriond Workshop*, edited by J. Tran Thanh Van, T. Damour, E. Hinds, and J. Wilkerson, Villars-Sur-Ollon, Switzerland, pp. 471–489, January 21–28, 1993.

[17] R. E. Best, *Phase-Locked Loops: Theory, Design, and Applications*, New York: MacGraw-Hill, 1984.

[18] T. Y. Otoshi and M. M. Franco, "Measurements of a Deep Space Station Fractional Frequency Stability to the 10^{-15} Level," *IEEE Trans. Instr. Measur.*, vol. 41, no. 5, pp. 577–587, 1992.

[19] J. B. Pollack, D. H. Atkinson, A. Seiff, and J. D. Anderson, "Retrieval of a Wind Profile From the Galileo Probe Telemetry Signal," *Space Science Reviews*, vol. 60, no. 8, pp. 143–178, 1992.

Appendix

The Radio System

In this Appendix, we provide a general description of the radio hardware shown in Fig. 2. For a more comprehensive analysis, the reader is referred to Footnote 2 and the references therein.

In Fig. 2, the H-maser and frequency distribution represent the overall contribution of the reference clock itself and the cabling system that takes the signal generated by the H-maser to the antenna. This can be located several kilometers away from the site of the maser, implying that a highly stable cabling system is required. It has been shown at JPL that optical-fiber cables would not significantly degrade the frequency stability of the signal generated by the maser.[10]

The transmitter chain includes all the frequency multipliers that are needed to generate the desired frequency of the transmitted radio signal, starting from the frequency provided by the maser. It also takes into account the radio amplifier and the extra phase delay changes occurring between the amplifier and the feed cone of the antenna. The noise due to the amplifier is the dominant one, and it has been characterized in Footnote 5 and [15].

The transponders are responsible for keeping the phase coherence between the incoming and outgoing radio signals on the spacecraft and the Earth. Their performance depends on the accuracy of the tracking of the uplink signal by the phase-locked loop and the noise floor and nonlinearities of its electronic components [17].[11]

The receiver chains at the ground and on board the spacecraft can be modeled as having white phase fluctuations. The contribution to the overall noise budget from the receiver chain on the ground was due until now to the cabling running from the feed of the antenna to the actual receiver. For the ground antenna, this long network of cables will be removed with the use of future beam-waveguide antennas. These new antennas will be implemented by the year 2000 by the NASA Deep Space Network [18]. The noise figure given for the receiver chain in Table 1 assumes that a beam-waveguide antenna will be used.

[10] A. L. Riley, op cit.

[11] A. L. Riley, op. cit.

The frequency fluctuations of the receiver chain on board the spacecraft are estimated to be smaller because of a simple cabling system. We have assumed, however, that the level of noise of the receiver chain on board is equal to the one on the ground.

Like the receiver chains, the thermal noise of the system has a white phase noise spectrum, and it is due to the finiteness of the signal-to-noise ratio in the Doppler tracking link [8]. Since the frequency is the derivative of the phase, we deduce that the one-sided power spectral density of the relative frequency changes goes as f^2.

A Doppler read-out system on board the spacecraft (denoted with the symbol $\bigotimes$ in Fig. 2) has already been built for the Galileo orbiter; it extracts Doppler data from a radio signal transmitted from the atmospheric probe in order to measure wind velocities on descent to Jupiter. The space-based radio technology, therefore, does not need to be developed [19].